

This article was downloaded by:

On: 22 January 2011

Access details: *Access Details: Free Access*

Publisher *Taylor & Francis*

Informa Ltd Registered in England and Wales Registered Number: 1072954 Registered office: Mortimer House, 37-41 Mortimer Street, London W1T 3JH, UK



## The Journal of Adhesion

Publication details, including instructions for authors and subscription information:

<http://www.informaworld.com/smpp/title~content=t713453635>

### <sup>1</sup>H NMR Imaging Study of Molecular Mobility in Silica-Filled, TBBS-Sulfur Vulcanized *Cis*-Polyisoprene

Carol M. Hill<sup>a</sup>; Jack L. Koenig<sup>a</sup>

<sup>a</sup> Department of Macromolecular Science, Case Western Reserve University, Cleveland, OH, USA

**To cite this Article** Hill, Carol M. and Koenig, Jack L.(1999) '<sup>1</sup>H NMR Imaging Study of Molecular Mobility in Silica-Filled, TBBS-Sulfur Vulcanized *Cis*-Polyisoprene', *The Journal of Adhesion*, 71: 2, 211 – 229

**To link to this Article:** DOI: 10.1080/00218469908014849

**URL:** <http://dx.doi.org/10.1080/00218469908014849>

PLEASE SCROLL DOWN FOR ARTICLE

Full terms and conditions of use: <http://www.informaworld.com/terms-and-conditions-of-access.pdf>

This article may be used for research, teaching and private study purposes. Any substantial or systematic reproduction, re-distribution, re-selling, loan or sub-licensing, systematic supply or distribution in any form to anyone is expressly forbidden.

The publisher does not give any warranty express or implied or make any representation that the contents will be complete or accurate or up to date. The accuracy of any instructions, formulae and drug doses should be independently verified with primary sources. The publisher shall not be liable for any loss, actions, claims, proceedings, demand or costs or damages whatsoever or howsoever caused arising directly or indirectly in connection with or arising out of the use of this material.

# $^1\text{H}$ NMR Imaging Study of Molecular Mobility in Silica-Filled, TBBS-Sulfur Vulcanized *Cis*-Polyisoprene\*

CAROL M. HILL and JACK L. KOENIG<sup>†</sup>

*Department of Macromolecular Science, Case Western Reserve University, 10900 Euclid Avenue, Cleveland, OH 44106-7202, USA*

*(Received 23 September 1998; In final form 21 April 1999)*

The interactions of silica in zinc-activated, sulfur-vulcanized *cis*-1,4 polyisoprene were characterized at the 75% cure state using  $^1\text{H}$  NMR imaging spectroscopy. Variables examined included silica loading, mixing conditions, and presence of additives, including a coupling agent and polyethylene glycol. Rheometer curves indicated a decrease in cure rate and cure state as silica was increased.  $^1\text{H}$  NMR imaging showed an increase in the  $T_2$  relaxation times, and a decrease in the proton spin density  $N(H)$  as the filler load increases. Mixing conditions did not affect the cure rate, cure state, or the average  $T_2$  relaxation time; however, the distribution of relaxation times broadened with poor mixing. The presence of a coupling agent increased the cure rate and cure state, as well as decreased the  $T_2$  relaxation times as compared with samples with the same silica level, but without coupling agent. Polyethylene glycol (PEG) had slightly higher average  $T_2$  relaxation times, and a slightly broader distribution as compared with the sample without PEG added.

**Keywords:** Vulcanized; silica; NMR imaging; mobility; surface agent; coupling agent; plasticizer

## INTRODUCTION

Silica has been shown to be a useful reinforcing filler in natural rubber because of its improvement in a number of performance properties

---

\*Presented at the 21st Annual Meeting of The Adhesion Society, Inc., Savannah, Georgia, USA, February 22–25, 1998.

<sup>†</sup>Corresponding author. Tel.: 216-368-4176, Fax: 216-368-4171, e-mail: jlk@po.cwru.edu

[1–8]. These advantages include tear strength, abrasion resistance, tear resistance, flex, heat resistance, hardness, and improved rolling resistance. As a result, silica has found increased usage in the rubber industry, including use in products such as shoe soles, engine mounts, wire coats, heavy service tires, as well as applications which require the use of colored rubber. However, due to its polar nature, silica does not mix well with the nonpolar rubber. As a result, coupling agents and other additives, such as amines or glycols, have been used with the silica to improve the silica-rubber interactions and to counteract the detrimental effects due to the adsorption of the curatives [1, 2, 5, 6, 17–19].

Particle size is an important variable in rubber reinforcement. The smallest particles provide the highest tensile, tear strength, and abrasion resistance [2]. Silica in rubber exists as agglomerates, and these agglomerate structures are affected by mixing conditions, and those materials that react with silanols [2]. Therefore, a poorly-mixed sample was studied in this experiment to determine the effect, if any, on the vulcanization chemistry.

Nuclear magnetic resonance imaging (NMRI) spectroscopy has been shown to be a useful research technique for both medical and non-medical applications [9–15]. The application of NMRI to solid samples has posed problems in the past due to the fact that the molecular motions are not rapid enough to reduce dipolar interactions and chemical shift anisotropy, both of which cause lower resolution and increased line widths. However, elastomeric materials have been successfully imaged with the conventional NMRI techniques because of the extensive reorientational motions of the molecules which minimize the above interactions. Swelling of the sample in a deuterated solvent is another way to increase the molecular motions and to improve the resolution in the images obtained.

When compared with other imaging techniques, NMRI has the advantage of being able to map several material parameters for the observed nuclei, such as diffusion processes, relaxation times, and spin density of the given nuclei. The NMR signal is a function of the local spin concentration (spin density), as well as the spin-lattice ( $T_1$ ) relaxation time, and the spin-spin relaxation time ( $T_2$ ) of the nuclei. When these relaxation times are different, the particular pulse sequence used in the collection of the image can be utilized to exploit

the differences and, hence, develop contrast in the image. The spin-spin relaxation time,  $T_2$ , is one of the most important parameters observable in the NMRI experiment because it is sensitive to the low-frequency motions that occur on the molecular level in the polymeric samples [10].

The most common pulse sequence used in NMR imaging today is the spin-echo pulse sequence [9], which is used to measure the spin-spin relaxation ( $T_2$ ) time. In this method, the NMR signal is measured at several different echo times at a given repetition time. The image is constructed by acquiring a series of projections that are differentiated from each other by a phase difference in the phase-encoding gradient. Each projection is created by a  $90^\circ$  pulse, which tips the magnetization vector into the  $xy$ -plane where it begins dephasing, followed by a  $180^\circ$  pulse, which refocuses the magnetization, at which time the data are collected. A gradient is applied along the  $x$ -axis for frequency encoding, which causes the spins to precess at different frequencies determined by their position in the static magnetic field. A gradient along the  $y$ -axis is applied for phase encoding of the data, and causes the spins to dephase at different rates. The gradient applied along the  $z$ -axis is used for determining the position and thickness of the slice that is being imaged. The data are then Fourier transformed in two dimensions to produce the image of the sample. The above process is repeated many times in order to obtain a sufficient signal-to-noise ratio.

The pixel intensity in the NMR image is determined by the amplitude of the spin-echo, which is given by the following Eq. (9)

$$I \sim N(H)[1 - \exp(-T_R/T_1)]_1 \exp(-T_E/T_2) \quad (1)$$

where  $N(H)$  is the proton spin density,  $T_R$  is the repetition time,  $T_E$  is the echo time,  $T_1$  is the spin-lattice relaxation time, and  $T_2$  is the spin-spin relaxation time. If the repetition time is greater than the longest  $T_1$  of the sample, then the  $\exp(-T_R/T_1)$  term reduces to zero, leaving the signal intensity proportional only to the  $T_2$  relaxation parameter [9].

$$I \sim N(H) \exp(-T_E/T_2) \quad (2)$$

If the sample is assumed to be homogeneous, Eq. (2) can be written as:

$$I \sim K \exp(-T_E/T_2) \quad (3)$$

where  $K$  is a constant that is proportional to the proton spin density,  $N(H)$ , of the sample and the scaling factor for the signal gain in the NMR spectrometer. Different echo times are used to determine the values for both  $K$  and  $T_2$ .

In this study, five spin-echo experiments were performed for each sample for the determination of the  $T_2$  relaxation time. Only the echo times were changed between each experiment for a given sample.

The focus of this study was to identify and characterize the effects that silica may have on the vulcanization reaction of zinc-activated, sulfur-cured *cis*-1,4 polyisoprene. Compounds with different levels of silica filler, as well as samples with poor mixing, coupling agent, and polyethylene glycol, were examined.

## EXPERIMENTAL

### Sample Preparation

The rubber used in this study is Natsyn 2200, a synthetic high-*cis*-1,4-polyisoprene. Five samples were prepared following a standard wire coat formulation with various amounts of silica, but no additives. Three other formulations were prepared to investigate the effect of mixing conditions, as well as that of additives. One of these contained 30 phr (parts per hundred parts of rubber) of silica, but was mixed poorly. Bis-(3-(Triethoxysilyl)-Propyl) Tetrasulfide, a silane coupling agent better known as Si-69 from the Dugussa Corporation, was used in another. Polyethylene glycol, PEG, was added in the final sample. Table I shows the sample designations, formulations, and processing conditions for all the samples used in this study. After being properly mixed in a two-stage mixing process involving a Banbury mixer and a double-roll mill, samples were first cured using a Monsanto ODR-100 oscillating disk rheometer at 320°F (160°C) with a special die that produced button-like samples, to obtain the characteristic rheometer cure curve. Fresh uncured material was then cured in a hydraulic press with a pressure of 22,000 pounds (10,000 kilograms) at 320°F (160°C)

TABLE I Formulations and processing conditions (all in units of parts per hundred (phr) rubber)

<i>Min</i>	<i>Banbury 1</i>	<i>AK1</i>	<i>AK2</i>	<i>AK3</i>	<i>AK4</i>	<i>AK5</i>	<i>AK6</i>	<i>AK7</i>	<i>AK8</i>
0'	NATSYN								
	2200	100	100	100	100	100	100	100	100
0.5'	Wingstay	1.00	1.00	1.00	1.00	1.00	1.00	1.00	1.00
0.5'	HiSil 255G	-	15	15	30	25	-	25	15
1.5'	HiSil 255G	-	-	15	30	20	-	20	15
1.5'	Si-69	-	-	-	-	-	-	3.38	-
3.0'	Calsol 510	-	-	-	-	-	-	7.23	-
3.0'	Stearic Acid	2.00	2.00	2.00	2.00	2.00	2.00	1.50	2.00
Dump after 4' at 145-150°C									
	Mill:								
0'	Sundex	3.00	3.00	3.00	3.00	3.00	3.00	-	3.00
0'	Zinc Oxide	8.00	8.00	8.00	8.00	8.00	8.00	4.00	8.00
0'	Sulfur	4.50	4.50	4.50	4.50	4.50	4.50	2.50	5.07
0'	Santocure NS	0.80	0.80	0.80	0.80	0.80	0.80	-	0.80
0'	MBTS	-	-	-	-	-	-	1.50	-
0'	DPG	-	-	-	-	-	-	0.88	-
0'	PEG	-	-	-	-	-	-	-	0.60
0'	HiSil 255G	-	-	-	-	-	30	-	-

Mix thoroughly. The batches were put back into the Banbury for 2 minutes after mixing on the mill. AK6 was mixed in the 2nd Banbury for only 30 seconds.

for the times corresponding to T75, which is 75% of the rheometer torque increase, according to the ODR-100 rheometer trace.

The cured rubber was swollen in chloroform for 24 hours, and cut using a circular punch to fit a 15 mm sample vial. The samples were then vacuum dried for 24 hours to remove the chloroform. Next, a Soxhlet extraction was performed in cyclohexane for 24 hours to remove all the non-network components. The samples were dried again to remove the protonated solvent. They were then transferred to a vial and reswollen in deuterated chloroform,  $\text{CDCl}_3$ , to equilibrium swelling, and stored in the deuterated solvent in a refrigerator at a temperature of approximately 5°C, until the imaging experiment was to be run. When the imaging experiments were run, the samples were removed from the vial, and placed in a 15 mm glass NMR tube between two Teflon spacers. The sample and the spacers were covered with  $\text{CDCl}_3$  to ensure that the rubber remained swollen throughout the measurements.

### Nuclear Magnetic Resonance Imaging

$^1\text{H}$  NMR images were acquired by a Bruker MSL 300 spectrometer at a resonance frequency of 300.13 MHz. A micro-imaging probe was used, in which a 15 mm sample vial was selected for the experiments. The images are  $256 \times 256$  pixels with a spatial resolution of 55  $\mu\text{m}$ . Thirty-two scans per phase-encode step were signal-averaged in producing each image, using a four-cycle phase routine ( $X, -Y, -X, Y$ ) and a recycle delay of 1 second.

The experiment used a spin-echo method, using a selective 90° pulse followed by a broad band 180° pulse for induction of the spin echo. Slice selection was performed by the use of a magnetic field gradient along the  $z$ -axis during the 90° pulse, and was approximately 1 mm. Magnetic field gradients were also employed along the  $x$ - and  $y$ -axes for frequency and phase encoding, respectively. The 90° pulse was 2000  $\mu\text{s}$  in length, while the 180° pulse was 90  $\mu\text{s}$  in duration. For each sample, five experiments were performed where the echo times ( $T_E$ ) were set to 9 ms, 10 ms, 12 ms, 14 ms, and 16 ms. Once the sample was placed into the NMR, only the echo time,  $T_E$ , was altered. All images were transferred to a SGI/UNIX workstation, and the data were processed using Tripes Image software.

The images for each batch were analyzed by scaling the pixel intensities to a common level for each of the samples in the batch. The pixels in the largest square area of the rubber region were averaged by the software. The average pixel intensity  $\langle I \rangle$  from within the swollen rubber region was expressed by:

$$\langle I \rangle = \langle K \rangle \exp(-T_E/\langle T_2 \rangle) \quad (4)$$

where  $\langle K \rangle$  is a constant that is proportional to the average proton spin density,  $N(H)$ , and  $T_2$  is the average  $T_2$  relaxation time of the rubber region. A plot was made of average pixel intensity *versus* echo time, and fit with the best fit linear line giving the slope, which was inversely proportional to the negative of the  $T_2$  relaxation time, and the intercept, which was the natural log of the constant,  $K$ , the proton spin density. The  $T_2$  relaxation time for each pixel was then calculated by:

$$T_2 = T_E/(\text{Ln}\langle K \rangle - \text{Ln} I_p) \quad (5)$$

where  $T_E$  is the echo time, and  $I_p$  is the intensity of the individual pixel. The  $T_2$  profile of relaxation times, where frequency (or number of pixels) was plotted against  $T_2$  relaxation time, was obtained by applying Eq. (5) to the 9 ms echo time intensity histogram obtained for each sample image.

## RESULTS

### Varying Silica Level

The MONSANTO ODR-100 recorded rheometer traces where torque was plotted against time for each of the varying silica levels. These curves can be found in Figure 1A. For the various silica levels, the curves were normalized by subtracting the minimum torque from each of the other points, to bring the minimum to zero, so that the torque effects due to the silica could be removed. These plots are shown in Figure 1B.

$^1\text{H}$  NMR proton spin images for the swollen, unfilled *cis*-polyisoprene are shown in Figure 2, and the images for one of the filled samples, 30 phr silica, is found in Figure 3. Not all of the images that were obtained are shown; the images shown are representative of the



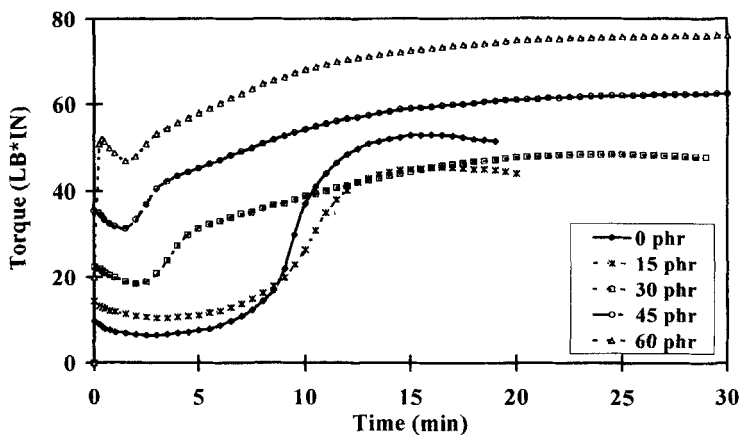


FIGURE 1A Monsanto ODR-100 rhcometer curves for varying silica loading.

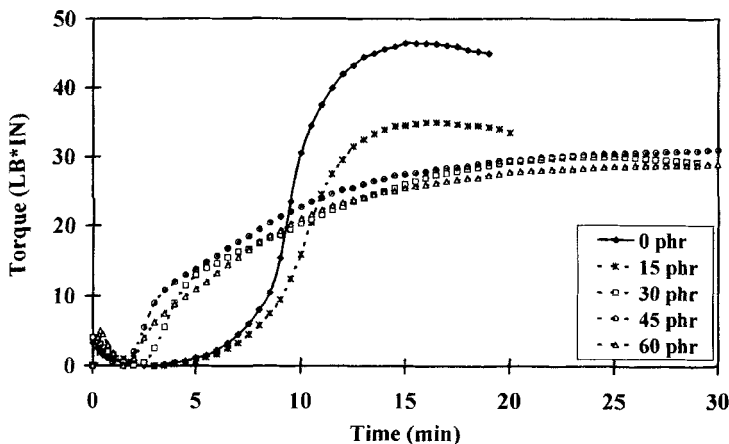


FIGURE 1B Normalized Monsanto ODR-100 curves for varying silica loading.

samples examined. The average pixel intensities inside the rubber region for all the samples are summarized in Table II. The color in the images is correlated with the mobility of the chains. The brighter the color in the image, the higher the signal intensity, which is related to higher mobility of the rubber chains.

The average  $T_2$  relaxation times were determined from the images, and are summarized for all the samples in Table III, as well as the constant,  $K$ , which is related to the proton spin density. The

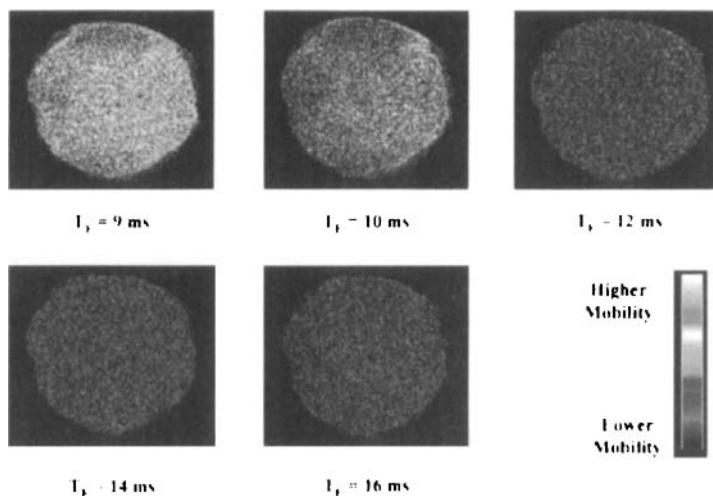


FIGURE 2  $^1\text{H}$  NMR images for unfilled *cis*-polyisoprene at various echo times. (See Color Plate I).

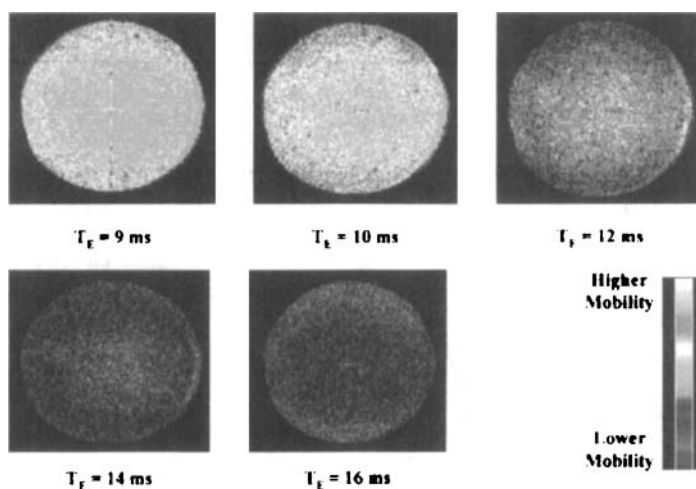


FIGURE 3  $^1\text{H}$  NMR images of 30 phr silica-filled *cis*-polyisoprene at various echo times. (See Color Plate II).

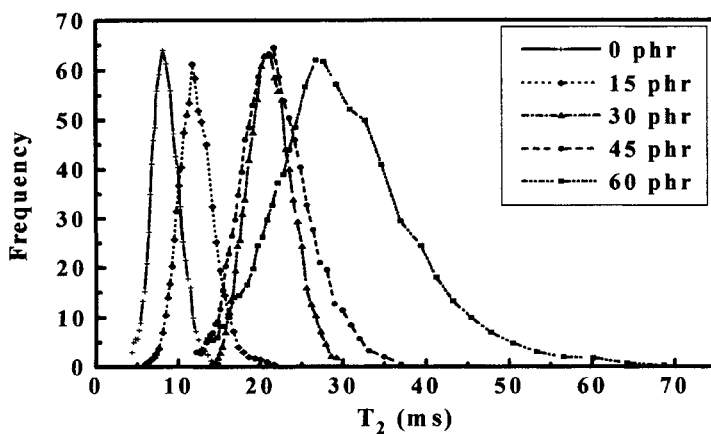
distribution of  $T_2$  relaxation times was calculated, and a plot of frequency (or number of pixels with the particular relaxation time) versus time was made for each sample, and can be found in Figure 4.

TABLE II Average pixel intensities for  $^1\text{H}$  NMR spin echo imaging experiments

Sample	Average intensity ( $\times 10^4$ )				
	$T_E = 9\text{ ms}$	$T_E = 10\text{ ms}$	$T_E = 12\text{ ms}$	$T_E = 14\text{ ms}$	$T_E = 16\text{ ms}$
AK 1	5.17	4.51	3.49	2.88	2.35
AK 2	5.69	5.21	4.51	3.95	3.50
AK 3	5.99	5.76	5.14	4.72	4.35
AK 4	6.91	6.56	5.95	5.39	4.98
AK 5	6.65	6.58	6.16	5.87	5.36
AK 6	8.35	7.92	7.10	6.52	6.02
AK 7	7.48	6.92	5.91	5.17	4.58
AK 8	7.75	7.38	6.74	6.14	5.73

TABLE III Average  $T_2$  relaxation times and proton spin density for varying silica loading

Sample	Amount silica (phr)	Average $T_2$ (ms)	Spin density ( $\times 10^4$ )
AK 1	0	8.94	13.83
AK 2	15	15.51	10.44
AK 3	30	21.46	9.09
AK 4	45	21.19	10.51
AK 5	60	32.79	8.86

FIGURE 4  $T_2$  relaxation time distribution curves for varying silica loading.

### Mixing Conditions

Rheometer curves for the sample with poor mixing were obtained from the Monsanto ODR-100, and compared with the sample that was well mixed. The mixing conditions did not greatly affect the rheometer traces.

$^1\text{H}$  images for the poorly-mixed sample are shown in Figure 5. Table II lists the average pixel intensities for the images. The  $T_2$  relaxation time distribution for the poorly-mixed sample is shown in comparison with the well-mixed sample in Figure 6. The overall  $T_2$  relaxation time for both is the same; however, the distribution for the sample that was poorly mixed is broader than for the sample that was well mixed.

### Additives: Si-69 Coupling Agent

The rheometer curves for the sample with coupling agent was obtained from the Monsanto ODR-100, and compared with the sample without coupling agent. The presence of coupling agent decreases the induction period and increases the cure rate dramatically, as can be seen by the

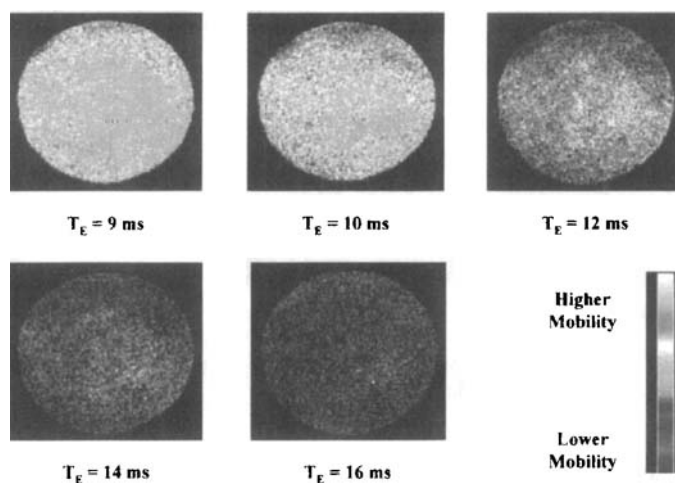


FIGURE 5  $^1\text{H}$  NMR images of poor mixing conditions in 30 phr silica-filled *cis*-polyisoprene at various echo times. (See Color Plate III).

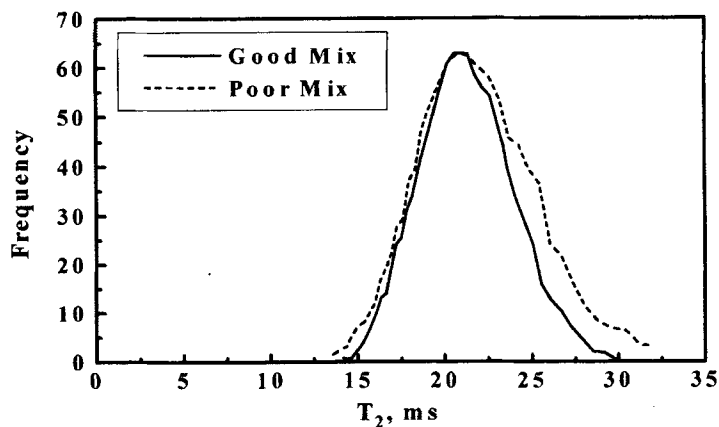


FIGURE 6  $T_2$  relaxation time distribution curves for samples with different mixing conditions. Both have 30 phr silica.

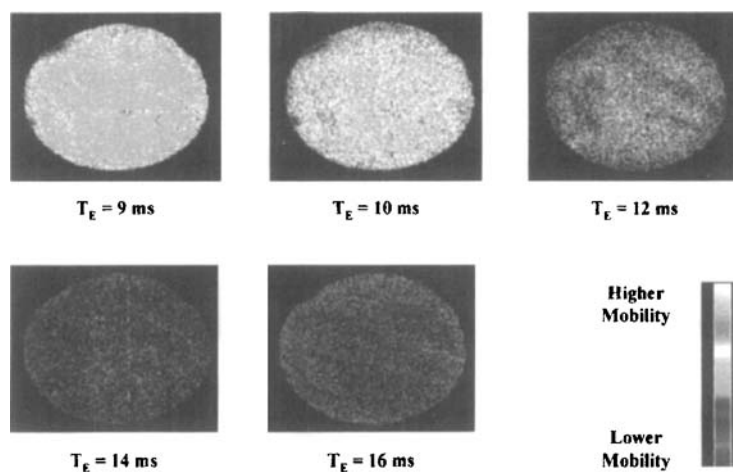


FIGURE 7  $^1\text{H}$  NMR images of 45 phr silica-filled *cis*-polyisoprene with coupling agent at various echo times. (See Color Plate IV).

rapid increase in the curve. At the 75% cure state, the sample with the coupling agent is at a higher torque, or cure state, than the sample without the coupling agent.

The  $^1\text{H}$  NMR images are shown in Figure 7 for the sample with coupling agent. Table II also lists the average pixel intensities for the

images obtained. The  $T_2$  relaxation time distribution for the sample with coupling agent is shown in Figure 8, where it was plotted with the sample with the same silica loading, but no coupling agent. The average  $T_2$  relaxation time with coupling agent decreased and the distribution became more narrow when coupling agent was used.

### Additives: Polyethylene Glycol (PEG)

The rheometer curve for the sample containing PEG was obtained from the Monsanto ODR-100, and compared with the sample without PEG. At low cure times, the sample with PEG has a much longer induction period, very much like the unfilled sample. However, at longer cure times, the rheometer curve follows that of the sample without PEG.

The  $^1\text{H}$  NMR images are shown in Figure 9 for the sample with PEG. Again, Table II lists the average pixel intensities for the images. Also, the  $T_2$  relaxation time distribution graph plotted for the sample without PEG is shown in Figure 10. The average  $T_2$  relaxation time did not change significantly with the addition of PEG but the distribution became slightly broader.

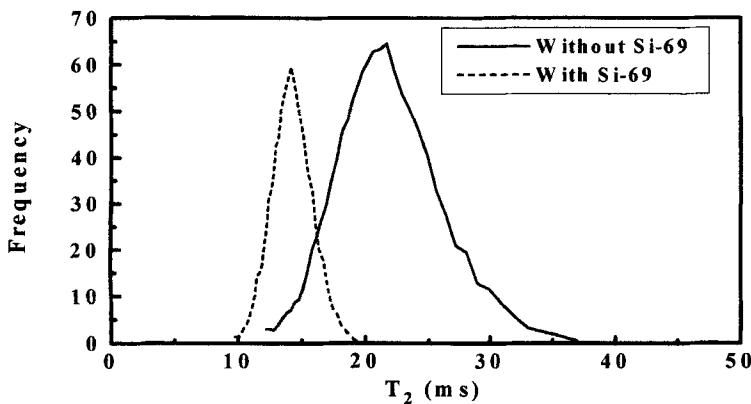


FIGURE 8  $T_2$  relaxation time distribution curves showing effect of adding coupling agent. Both have 45 phr silica.

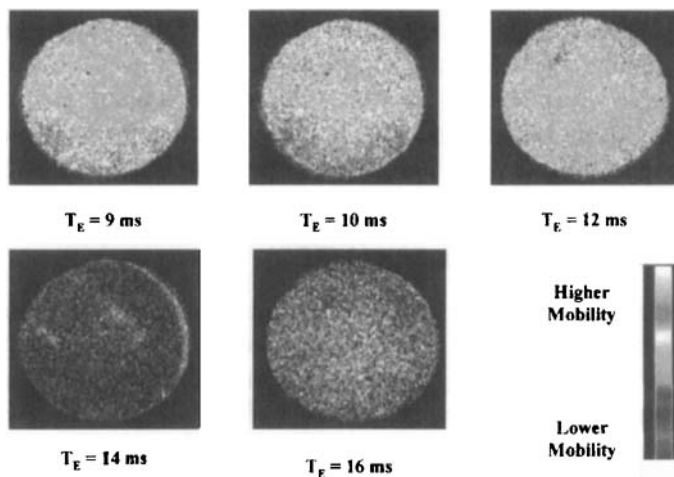


FIGURE 9  $^1\text{H}$  NMR images of 30 phr silica-filled *cis*-polyisoprene with polyethylene glycol (PEG) at various echo times. (See Color Plate V).

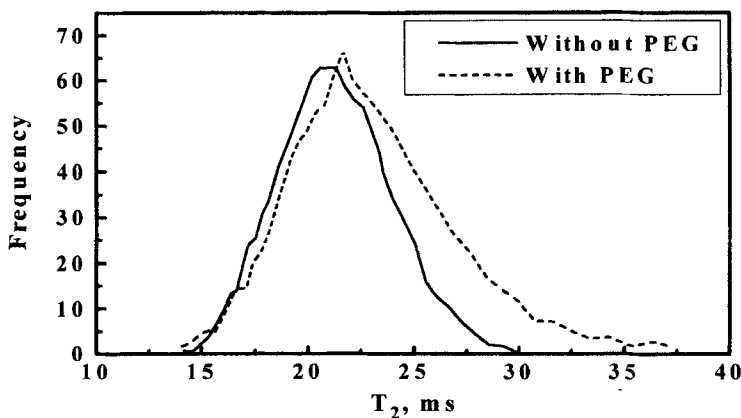


FIGURE 10  $T_2$  relaxation time distribution curves for samples with and without polyethylene glycol (PEG). Both have 30 phr silica.

## DISCUSSION

### Varying Silica Levels

The rheometer curves show a number of differences when silica is added as a filler in natural rubber. Firstly there is a change in the shape of the curve as the silica level is increased from 15 phr to 30 phr,

indicating that the curing rate is retarded by the addition of silica. There appears to be a change in the slope of the curves after a given inflection point. Silica has been shown to adsorb the cure ingredients [1]. Therefore, the change in slope of the rheometer curves has been attributed to the fact that the silica has adsorbed some of the cure ingredients. During the curing procedure, the cure ingredients that had been adsorbed must first desorb from the silica surface before they can react and cure the rubber. Therefore, the first part of the rheometer curve is the reaction of the non-adsorbed material, where the reaction is fast. Once the "free" curatives are used up, the remaining curatives must desorb from the surface of the silica, and then react to form the chemical crosslinks. This desorption process is much slower; therefore, the cure rate is slowed down. This effect produces the change in the slope of the rheometer traces. Fourier transform infrared (FTIR) spectroscopy measurements support this desorption theory, and the results are reported elsewhere [18].

Secondly, the initial torque measured by the rheometer increases as silica level increases. This occurs because the more silica there is, the stiffer the rubber and, therefore, the more resistance to torque that is experienced. The curves were normalized by subtracting the minimum torque from each of the various points on the curve. This brought the minimum to zero. This treatment of the data effectively removes the physical reinforcing effects of the silica, and allows for examination of the overall cure state of the rubber. As can be seen in Figure 1B, there is an overall decrease in the maximum torque achieved after normalization as silica is increased. This indicates that there are fewer crosslinks formed when silica is added, thus indicating that a lower cure state exists as more silica is added. This result is supported by Wolff who reported that the silica interferes with the vulcanization mechanism in sulfur-cure systems, reducing the crosslink yield [17], and by Hewitt, who states that silica removes the zinc from the accelerator complex, thus reducing the cure rate and cure state [2].

Finally, there is a reduction in the induction period as more silica is added. The differences in the induction period among the five formulations is attributed to the differences in the individual thermal histories. The heat generated in the system during mixing increases with increasing filler content, thereby causing the possibility of some vulcanization occurring during the mixing process. Additionally, in the review of sulfur vulcanization chemistry by Krejsa and Koenig [16] it



was found that the scorch delay and the vulcanization rate were controlled by the accelerator/sulfur ratio. Since silica has been found to adsorb the curatives, especially zinc and the accelerator [1], the accelerator/sulfur ratio would decrease as more silica was added, due to the added adsorption of the accelerator. The end result would be a decrease in the scorch delay as more silica is added, as observed in these experiments. (Scorch delay is the delayed cure after the maximum of the cure rate is achieved.)

From the imaging studies, it was determined that the average  $T_2$  relaxation times increased as the silica increased, as seen in Figure 4. The  $T_2$  relaxation times are sensitive to the low frequency motions of the polymer chains. Therefore, an increase in the  $T_2$  relaxation times would indicate more mobility of the polymer chains. From the imaging studies, it can be concluded that as silica is increased, the average  $T_2$  relaxation times increases, indicating more mobile rubber chains and, therefore, a lower cure state.

It was also found that the distribution of  $T_2$  relaxation times becomes broader as more silica was added. This can be explained by the fact that as more silica is added, there is more adsorption of the curatives, and more inherent inhomogeneity in the sample. Therefore, the distribution of the  $T_2$  relaxation components increases.

### Mixing Conditions

There was very little difference observed between the rheometer traces for the poorly-mixed and well-mixed samples. This indicates that mixing conditions do not affect the overall cure rate and cure reaction.

The NMR imaging results indicated that the overall  $T_2$  relaxation time for both samples remained the same. The only difference arose when comparing the breadth of the distribution. The poorly-mixed sample had a broader  $T_2$  relaxation time distribution, indicating less homogeneity in the sample. The poorly-mixed silica would form large and irregular agglomerates that were not broken up during mixing, thus causing less homogeneous samples. The result of this would be a broader distribution of  $T_2$  relaxation components throughout the sample, showing up in the NMR images.

### **Additives: Si-69 Coupling Agent**

Coupling agents are added in order to improve the rubber–silica interactions, and to promote better mixing of the silica in the rubber. Adding the coupling agent significantly affects the rheometer curves, in both shape and time scale. The induction period decreased dramatically and the cure rate increased significantly when coupling agent was added. The shape also changed, as mentioned, which indicates that the coupling agent prevents the silica from adsorbing the curatives. The cure curve has the typical shape for unfilled isoprene rubber, in which there can be no adsorption of the curing agents. As mentioned before, the cure curve for the sample without the coupling agent has the double slope characteristic of the adsorption of the curatives.

The imaging results showed that the  $T_2$  relaxation time decreased when coupling agent was added as compared with the sample without coupling agent. This indicates that the mobility of the rubber chains is restricted when coupling agent is added, as compared with the sample without coupling agent. The restricted motion can be attributed to a higher cure state in which the sulfur crosslinks restrict the chain motions. A higher cure state may exist due to the fact that the coupling agent reacts with the silica preferentially, thus preventing the adsorption of the curatives, thereby allowing for a normal cure reaction. One end of the coupling agent molecule reacts with the polar silica and the other end reacts with the non-polar rubber and, as a result, better interactions between the silica and the rubber develop, thereby restricting the motion of the isoprene chains.

### **Additives: Polyethylene Glycol**

The rheometer traces for the sample with PEG added showed an increase in the induction period at low cure times. There is also a larger region of “free” curatives, before the curve takes on the large change in slope, indicating a retarded cure rate. At longer cure times, however, the differences between the two curves decreased and the curves became very similar. The changes in the early portions of the curves indicate that the PEG is coating the surface of the silica and reducing the amount of adsorption of the cure agents. However, the fact that the rheometer

curve shifts back to the shape of the sample without PEG indicates that the PEG did not prevent all of the curatives from being adsorbed. There was some adsorption and, therefore, there was some desorption of the curatives during the cure, resulting in the slower cure rate. At longer cure times, there was very little difference between the two curves.

The  $T_2$  relaxation distribution curves shown in Figure 10 show small differences. The imaging samples were at the 75% cure state. As mentioned above, at later stages of cure, the samples differed only slightly. Therefore, the  $T_2$  relaxation distribution times should differ only slightly, which was that was observed. The width of the  $T_2$  distribution curve was slightly larger, indicating a sample that was slightly less homogeneous than the sample without PEG.

## CONCLUSIONS

Silica has been shown to retard the cure reaction, and reduce the cure state when it is used as a filler in *cis*-1,4 polyisoprene, without additional processing aids like coupling agent or polyethylene glycol. The mixing conditions do not seem to affect the cure rate or cure state. However, poor mixing results in less homogeneous samples and a broader distribution of  $T_2$  relaxation times. Coupling agent increased the cure rate and the cure state. It also reduced the distribution of  $T_2$  relaxation times throughout the sample, thus indicating a more homogeneous sample. Polyethylene glycol (PEG) increased the induction period, and reduced the amount of adsorbed curatives at an early stage of cure. However, at longer cure times, the samples were the same. PEG also did not significantly affect the  $T_2$  relaxation time distribution in samples as compared with samples without PEG but with the same level of silica filler.

## References

- [1] Wagner, M. P., *Rubber Chem. Technol.* **49**, 703 (1976).
- [2] Hewitt, N. L., "An Introduction to Silica Fillers", paper presented at the meeting of the Rubber Division of the American Chemical Society, Philadelphia, Pennsylvania, May 1995.
- [3] Okel, T. A. and Waddell, W. H., *Rubber Chem. Technol.* **67**, 217 (1994).
- [4] Evans, L. R. and Waddell, W. H., *Rubber and Plastic News* (April 25, 1994).

- [5] Waddell, W. H., Evans, L. R. and Okel, T. A., *Tire Technology International* 22 (1994).
- [6] Waddell, W. H., Beauregard, P. A. and Evans, L. R., *Tire Technology International* 24 (1995).
- [7] Okel, T. A. and Waddell, W. H., *Rubber Chem. Technol.* **68**, 59 (1995).
- [8] Waddell, W. H. and Evans, L. R., *Rubber Chem. Technol.* **69**, 377 (1996).
- [9] Koenig, J. L., In: *Spectroscopy of Polymers* (American Chemical Society, Washington, DC, 1992), Chap. 11.
- [10] Komoroski, R. A., *Anal. Chem.* **65** (24), 1068A (1993).
- [11] Krejsa, M. R. and Koenig, J. L., *Rubber Chem. Technol.* **64**, 635 (1991).
- [12] Chang, C. and Komoroski, R. A., *Macromolecules* **22**, 600 (1989).
- [13] Smith, S. R. and Koenig, J. L., *Macromolecules* **24**, 3496 (1991).
- [14] Liu, J., Nieminen, A. O. K. and Koenig, J. L., *J. Mag. Res.* **85**, 95 (1989).
- [15] Mori, M., *Ph.D. Thesis*, Case Western Reserve University, Cleveland, Ohio, 1997.
- [16] Krejsa, M. R. and Koenig, J. L., *Rubber Chem. Technol.* **66**, 376 (1993).
- [17] Wolff, S., *Rubber Chem. Technol.* **69**, 325 (1996).
- [18] Kraleovich, M. L. and Koenig, J. L., *Rubber Chem. & Tech.* **71**, 300–309 (1998).
- [19] Fetterman, M. Q., *Elastomerics* **116**, 18 (1984).